



How Rainfall Events Modify Trace Gas Concentrations in Central Amazonia

Luiz A. T. Machado^{1,2}, Jürgen Kesselmeier¹, Santiago Botía³, Hella van Asperen³, Alessandro C. de Araújo⁴, Paulo Artaxo², Achim Edtbauer¹, Rosaria R. Ferreira⁵, Hartwig Harder¹, Sam P. Jones³, Cléo Q. Dias-Júnior⁶, Guido G. Haytzmann², Carlos A. Quesada⁵, Shujiro Komiya³, Jost Lavric^{3,15}, Jos Lelieveld^{1,7}, Ingeborg Levin⁸, Anke Nölscher^{1,16}, Eva Pfannerstill^{1,17}, Mira M. Pöhlker^{1,9,10}, Ulrich Pöschl¹, Akima Ringsdorf¹, Luciana Rizzo², Ana M. Yáñez-Serrano^{11,12,13}, Susan Trumbore³, Wanda I. D. Valenti⁵, Jordi Vila-Guerau de Arellano¹⁴, David Walter^{1,3}, Jonathan Williams¹, Stefan Wolff^{1,18}, and Christopher Pöhlker¹

¹ Max Planck Institute for Chemistry, 55128 Mainz, Germany

² Instituto de Física, Universidade de São Paulo, São Paulo, Brazil

³ Max Planck Institute for Biogeochemistry, Jena, Germany

⁴ Embrapa Amazônia Oriental, Belém, PA, Brazil

⁵ Instituto de Pesquisas da Amazonia, INPA, Manaus, Brazil

⁶ Department of Physics, Federal Institute of Pará, Belém, PA, Brazil

⁷ The Cyprus Institute, Climate and Atmosphere Research Center, Nicosia, 1645, Cyprus

⁸ Institut für Umweltphysik, Heidelberg University, Heidelberg, Germany

⁹ Faculty of Physics and Earth Sciences, Leipzig Institute for Meteorology, University of Leipzig, Leipzig, Germany

¹⁰ Experimental Aerosol and Cloud Microphysics Department, Leibniz Institute for Tropospheric Research, Leipzig, Germany

¹¹ Instituto de Diagnóstico Ambiental y Estudios del Agua (IDAEA), Barcelona, Spain

¹² Centro de Investigación Ecológica y Aplicaciones Forestales (CREAF), Catalonia, Spain

¹³ Global Ecology Unit (CREAF-CSIC-UA), Catalonia, Spain

¹⁴ Meteorology and Air Quality Section, Wageningen University, The Netherlands

¹⁵ Acoem GmbH, Hallbergmoos, Germany

¹⁶ University of Bayreuth, Bayreuth, Germany

¹⁷ Institute of Energy and Climate Research, Jülich, Germany

¹⁸ German Weather Service, 63067 Offenbach, Germany

Correspondence: Luiz A. T. Machado (l.machado@mpic.de)

Abstract. This study investigates the rain-initiated mixing and variability in the concentration of selected trace gases in the atmosphere over the central Amazon rain forest. It builds on comprehensive data from the Amazon Tall Tower Observatory (ATTO), spanning from 2013 to 2020 and comprising the greenhouse gases (GHG) carbon dioxide (CO₂) and methane (CH₄), the reactive trace gases carbon monoxide (CO), ozone (O₃), nitric oxide (NO), and nitrogen dioxide NO₂ (NO₂) as well as selected volatile organic compounds (VOC). Based on more than 1000 analyzed rainfall incidents, the study resolves the trace gas concentration patterns before, during, and after the rain events, along with its vertical concentration gradients across the forest canopy. The assessment of the rainfall events was conducted independently for daytime and nighttime periods, which allows us to elucidate the influence of solar radiation. The concentrations of CO₂, CO, and CH₄ clearly declined during rainfall, which can be attributed to the downdraft-related entrainment of pristine air from higher altitudes into the boundary layer, a reduction of the photosynthetic activity under increased cloud cover, as well as changes in the surface fluxes. Notably,



CO showed a faster reduction than CO₂, and the vertical gradient of CO₂ and CO is steeper than for CH₄. Conversely, the O₃ concentration increased across all measurement heights in the course of the rain-related downdrafts. Following the O₃ enhancement by up to a factor of two, NO and VOC concentrations decreased, whereas NO₂ increased. The temporal and vertical variability of the trace gases is intricately linked to the diverse sink and source processes, surface fluxes, and free troposphere transport. Within the canopy, several interactions unfold among soil, atmosphere, and plants, shaping the overall dynamics. Also, the concentration of biogenic VOC (BVOC) clearly varied with rainfall, driven by factors such as light, temperature, physical transport, and soil processes. Our results disentangle the patterns in trace gas concentration in the course of the sudden and vigorous atmospheric mixing during rainfall events. By selectively uncovering processes that are not clearly detectable under undisturbed conditions, our results contribute to a better understanding of the trace gas life cycle and its interplay with meteorology, cloud dynamics, and rainfall in the Amazon and beyond.



A precise understanding of the interaction between the atmosphere and the forest is crucial to accurately simulate and predict the effects of climate and land use change in Amazonia. Atmospheric multiphase processes and chemical reactions are mainly controlled by the concentration of reactive gases and governed by rainfall, thermodynamics, and solar radiation (Ravishankara, 1997). Rainfall events can significantly impact these processes by causing sudden and quite strong changes in trace gas concentrations over short periods of time (Bertrand et al., 2008). Therefore, it is essential to understand how weather conditions affect the interaction between the atmosphere and the biosphere to develop comprehensive parameterizations for climate models. The Amazon Tall Tower Observatory (ATTO) is a well-equipped site with laboratories and towers. The essential element is a tall tower (325 meters) equipped with a wide range of micrometeorological and trace gas sensors. The so-called Instant and Triangle Towers were erected in 2012, each with a height of 80 meters; see Andreae et al. (2015) for a detailed description of the ATTO instrumentation. These towers have been monitoring gas concentrations since then, serving as the primary data source for this study. The data collected at ATTO has been invaluable in advancing our knowledge of the atmosphere-biosphere interaction. Numerous studies have been published using the ATTO data and contributed to our understanding of processes such as particle formation (e.g., Machado et al., 2021; Franco et al., 2022; Pöhlker et al., 2016; Moran-Zuloaga et al., 2018) and long-range transport (e.g., Holanda et al., 2020, 2023), as well as biogenic gases and particles (e.g., Kesselmeier and Staudt, 1999). The journal Atmospheric Chemistry and Physics features a specialized volume devoted to ATTO research (Amazon Tall Tower Observatory (ATTO) Special Issue), comprehensively analyzing the intricate physical, chemical, and biological interactions inherent in the Amazon rain forest.

The factors influencing the temporal variability of greenhouse gas (GHG) measurements have been studied widely. The global trend of the atmospheric growth rate of carbon dioxide (CO₂) (Lan et al., 2023) and methane (CH₄) (Thoning et al., 2022) has been documented extensively by global measurement networks, revealing accumulation of these trace gases in the atmosphere. The temporal patterns at a particular measurement site are embedded in this global trend but follow seasonal and diurnal patterns specific to their latitude and local drivers. On a tall tower at a boreal forest site in Siberia, the so-called ZOTTO-site, fluxes and concentrations of carbon monoxide (CO), CO₂ and CH₄ were extensively monitored for more than a decade as reported by Panov et al. (2022), showing seasonal and diurnal variations, driven by the growing season and type of vegetation, such as seasonally flooded wetlands. At the ATTO site, the seasonal pattern of nighttime CH₄ peaks at the 79-m level was described by Botía et al. (2020), highlighting the atmospheric conditions for these events and the potential sources from which these CH₄ enhancements could be coming from. Using a Lagrangian model to obtain the background concentration of CO₂ at ATTO (79-m), Botía et al. (2022) derived the regional signal (observations - background) of CO₂ and found that the amplitude of the seasonal cycle was of about 4 ppm. In that study they also show how the atmospheric record captured the CO₂ anomalies caused by the 2015/2016 El Niño-induced drought. At the diurnal cycle scale, the changes in atmospheric trace gases result from the interaction between local factors and the dynamics and subsequent growth of the planetary boundary layer (PBL). For gases such as CH₄, ozone (O₃), and nitrogen dioxide (NO₂), Mikkilä et al. (1995) found a relationship between soil temperature, solar radiation, and diurnal emission variability. CH₄ exhibits inter-annual variability and a trend of increasing concentration, the background of which is still not understood (Rigby et al., 2017; Schaefer et al., 2016; Nisbet et al., 2019).



55 Given these studies, the drivers of inter-annual, seasonal, and diurnal variability of trace gases in the atmosphere are part of a wide range of processes that include atmospheric dynamics and chemistry, but so far, a study of the immediate influence of rain events is lacking.

[Williams et al. \(2001\)](#) conducted some of the earliest studies on time-space variability of trace gases in the Amazon forest and observed large spatial and temporal variability of gas concentration, resulting in strong gradients of CO and CO₂ concentrations. [O₃](#) is strongly modulated by environmental variables, such as rainfall and the transport of ozone-rich air in the free atmosphere, as described by [Betts et al. \(2002\)](#); [Gerken et al. \(2016\)](#); [Machado and all \(2023\)](#). Lighting can also increase O₃ concentrations, as discussed by [Shlanta and Moore \(1972\)](#). The hydroxyl radical (OH), an oxidative component acting as a sink for volatile organic compounds (VOCs) ([Pfannerstill et al., 2021](#)), and a catalyst for the further reactions of different trace gases in rain-forest, is strongly modulated by environmental variables, including rainfall, temperature, and radiation ([Nölscher et al., 2016](#); [Ringsdorf et al., 2023](#)), and exhibits important vertical stratification and variations on intradiurnal to interannual scales.

VOCs are reactive atmospheric trace gases and comprise many groups of saturated, unsaturated, and oxygenated derivatives ([Kesselmeier and Staudt, 1999](#)). Biogenic VOCs (BVOC) include isoprenoids (isoprene and monoterpenes) as well as alkanes, alkenes, carbonyls, alcohols, esters, ethers, and acids. Their reactivities are high, and their lifetimes in the atmosphere range from < 1 min to days. Some species are hardly detectable under normal atmospheric conditions as they react too fast with O₃ and radicals. Thus, BVOCs exhibit highly dynamic fluctuations with strong diurnal and seasonal characteristics. For an overview, see [Kesselmeier and Staudt \(1999\)](#) and [Yanez-Serrano et al. \(2020\)](#). Atmospheric concentrations strongly depend on atmospheric oxidation processes, but the anthropogenic and biogenic production and emission pathways should never be overseen. As reported by [Laothawornkitkul et al. \(2009\)](#), BVOCs are produced in the course of many plant physiological and metabolic pathways involved in plant growth, development, reproduction, and defense. Their release into the atmosphere depends on solubility and volatility and can, therefore, depend on and independent from physiological gas exchange regulation under stomatal control. Some of the BVOC species are released close to the concentration gradient between outside air and plant tissue; some are under strict stomatal control. This behavior strongly depends on water solubility, i.e., equilibrium gas–aqueous phase partition coefficient [Niinemets \(2007\)](#). Thus, emission can occur in different manners, from constant diffusion to sudden bursts. Within this context, we have to consider climate, season, and diurnal effects to include plant adaptation and development as well as physiological reactions on shorter time scales, as slow and fast changes of BVOC emission in relation to adaptation and developmental processes for plants, soil, and leaf litter. Within this context, bursts of gases and aerosols are often observed during and after rain events ([Greenberg et al., 2012](#); [Bourtsoukidis et al., 2018](#); [Rossabi et al., 2018](#)). Such emission bursts, or upward air mass transport, can be responsible for sudden changes in the OH-reactivity ([Pfannerstill et al., 2021](#)).

85 This study aims to provide a comprehensive overview of the fluctuations in trace gas concentrations due to rainfall events occurring within and immediately above the canopy at a site that serves as a representative sample of the central Amazon region.



We analyzed these fluctuations in relation to rainfall events during the day and night. Long-term measurement profiles enable us to analyze the interaction between soil, canopy, and boundary layer to specifically assess how the profile of greenhouse and reactive gases vary before, during, and after rainfall events.

90 1 Data and Methodology

1.1 Measurement systems

This study utilizes the greenhouse gases (GHG) and reactive gases concentration data collected at the Instant tower at different heights with diverse instrumentation. For the gases NO_x (nitric oxide (NO) and NO₂) and O₃, the data for this study was collected between 2013 and 2020 (for O₃) and between 2018 and 2020 (for NO and NO₂), and monitored concentrations at the
95 heights 0.05, 0.5, 4, 12, 24, 38, 53, and 79 m, where 0.05 m hovers just above the surface, and 79 m is elevated approximately 40 m above the canopy. Each height was measured 4 times per hour, and air was sampled directly from the inlet height. Timestamps were rescaled to 30-minute intervals for each altitude. The concentrations of NO_x (NO and NO₂) and O₃ were acquired using an Eco Physics CLD TR 780 and a Thermo Scientific 49i O₃ Analyzer, which measured by UV photometry with a precision of 1 ppb, respectively, as referenced in [Andreae et al. \(2015\)](#). Employing a gas-phase chemiluminescence
100 technique, the CLD measurements precisely captured the NO mixing ratio with a precision better than 25 ppt. Subsequently, NO₂ was determined by converting it to NO through a photolytic converter driven by UV radiation (Solid-state Photolytic NO₂ Converter (BLC); DMT, Boulder/USA). Regular calibration was conducted with a Dynamic Gas Calibrator.

For CO, CO₂ and CH₄, the data for this study was collected between 2013 and 2020. Sample air from five different heights (4, 24, 38, 53, and 79 m) was led through a buffer system, such as described by [Winderlich et al. \(2010\)](#), which was connected to
105 two state-of-the-art instruments, employing cavity ring-down spectroscopy, specifically with the G1301 and G1302 analyzers (Picarro Inc.). The G1301 analyzer (serial number CFADS-109) consistently delivers data with remarkable precision, displaying a minimal standard deviation of less than 0.05 ppm for CO₂ and 0.5 ppb for CH₄ in the raw readings. Furthermore, the device exhibits exceptional stability over time, with a long-term drift of under 2 ppm for CO₂ and 1 ppb annually for CH₄. The G1302 analyzer, identified by the serial number CKADS-018, underwent rigorous testing using a stable gas tank. This com-
110 prehensive assessment revealed a standard deviation of 0.04 ppm for CO₂ and 7 ppb for CO in the raw data. Both instruments automatically measured 3 calibration gases every 100 hours, and a target tank every 30 hours. The measurement strategy was to cover all heights four times per hour, with a resampling rate of 30 minutes.

Isoprene (C₅H₈) and monoterpenes (C₁₀H₁₆) were collected at the instant tower, using a Proton Transfer Reaction Mass Spectrometer (PTR-MS) during several campaigns between November 2012 to December 2015. Concentrations were measured at
115 0.05, 0.5, 4, 12, 24, 38, 53, and 79 m, where the canopy top is between 24 and 38 m. The sample inlets (3/8"OD insulated Teflon) were connected to the PTR-MS and installed at the foot of the instant tower. Each level of the vertical profile was sampled every 2 minutes between different heights. This sequential operation allowed for a complete profile to be generated in



just 16 minutes. The measurements were focused on two compounds: isoprene (m/z 69.069) and monoterpenes (m/z 137.132). For a detailed description, see [Yáñez Serrano et al. \(2015\)](#) and [Yanez-Serrano et al. \(2020\)](#). All trace gas profiles were linearly
120 interpolated in 5-meter steps from the surface to 80 meters for better visual quality and equal vertical distribution.

The air temperature, relative humidity, pressure, precipitation, wind speed, and solar radiation were measured using weather sensors installed at the instant tower. Temperature and relative humidity were measured using a Termo-hygrometer (CS215, Rotronic Measurement Solutions, UK), rainfall was obtained using a Raingauge (TB4, Hydrological Services Pty. Ltd., Australia), the wind speed was obtained through a 2-D sonic anemometer (WindSonic, Gill Instruments Ltd., UK) and the solar
125 radiation with a Net radiometer (NR-LITE2, Kipp-Zonen, Netherlands). The data was collected from 2013 to 2020, but the parameters experienced intermittent failures at various times. From ABI (Advanced baseline imager) channel 13, total cloud cover was estimated, collocated at the ATTO site as the frequency of occurrence of brightness temperature (T_{IR}) $<$ 284 K following [Machado et al. \(2021\)](#). The GLM (Geostationary Lightning Mapper) events, describing the lightning activity, were obtained from the GOES-16 GLM sensor, also collocated at ATTO site as the number of events every ten minutes in an area
130 of 5 by 5 in a 25 km radius, similar to [Machado et al. \(2021\)](#). T_{IR} as well as GLM events were resampled every 30 minutes. Boundary layer heights were measured using a ceilometer model CHM15k (Jenoptik AG, Jena, Germany). The ceilometer is an instrument based on LIDAR, which involves capturing the intensity of optical backscatter in the wavelength range 900-1100 nm by emitting autonomous vertical pulses. LIDAR measurements are reliant on aerosol concentrations in the atmosphere. Within the PBL, aerosol concentrations are notably higher compared to the free atmosphere above, and this contrast serves
135 as the foundation for detecting the PBL height through LIDAR measurements, see [Dias-Júnior et al. \(2022\)](#). Boundary layer height data were resampled every 30 minutes from 2014 to 2020.

^{222}Rn is a naturally occurring radioactive noble gas of terrestrial origin and is produced via the decay of long-lived radium isotope ^{226}Ra , present in most rock and soil types ([Nazaroff, 1992](#)). ^{222}Rn is measured in $\text{Bq}\cdot\text{m}^{-3}$, corresponding to the amount of radon radioactive decay per second in a volume of air and is used as a proxy of surface-atmospheric mixing and transport.
140 ^{222}Rn and CO_2 undergo similar exchange processes between the soil and the atmosphere, and all trace gases experience comparable atmospheric mixing phenomena as atmospheric mixing is turbulent. The flow of ^{222}Rn can be considered almost constant in the absence of rain and changes in pressure. Consequently, it can serve as a proxy for assessing the dynamics of CO_2 emission/sink from/to the soil ([Hirsch, 2007](#)). Atmospheric radon activity concentration was measured at 80 m on the ATTO tall tower. This study's data period ranges from January 2019 to December 2020. The measurement used a static filter
145 collecting radon progeny on a filter method and assuming radioactive equilibrium between atmospheric radon and its daughters as described by [Levin et al. \(2002\)](#), and a correction was made to account for the aerosol loss in the intake line as presented in [Levin et al. \(2017\)](#). The data was combined with rainfall to produce a composite for day and night to evaluate the relative importance of surface fluxes on the changes of the gas concentration during rainfall events. The radon source can be assumed to be approximately constant over the diurnal cycle and horizontally uniform on local scales ([Nazaroff, 1992](#)). One limitation
150 of this measurement is the error associated with situations where the relative humidity is larger than 95% or during rain events,



when part of the atmospheric radon progeny may have been lost due to scavenging effects. In these situations, the general assumption that progeny are in equilibrium with the radon gas may be violated. To avoid this imprecision, the measurements used in this study account for only cases where the relative humidity is smaller than this threshold and are only applied for the range of two hours before the time of maximum rain.

155 1.2 Data analysis

We conducted a composite study following the same methodology as [Machado et al. \(2021\)](#), in which composites were based on the time of maximum rainfall events. This study intends to analyze the gas concentration evolution during rainfall events by selecting moments within 4-hour time slots and using composite analysis to obtain the medium pattern evolution before and after maximum rainfall. Composite analyses are useful to study physical hypotheses that occur over time ([Boschat et al., 2016](#)). This method quantifies standardized instances of a specific phenomenon, such as a rainfall event, and consolidates them into a composite. In this study, we computed the gas concentration during rainfall events with a maximum rain rate inside the four-hour time slot as the reference time. This analysis considered a time frame spanning two hours before and after the peak rain rate. A rainfall event was defined as any instance where the rain rate exceeded 0.5 mm.hr^{-1} within a 4-hour window, with the peak occurring at the moment of maximum rain rate. We evaluated the composites at three distinct time points: at the onset, at the end of the rain event, and the moment of peak rainfall intensity. The results exhibited qualitative similarity in gas concentration evolution across these different calculations, except for gas concentration at the moment designated as the reference time. We specifically chose the moment of maximum rain rate as the reference time to center the composite analysis on the most intense phase of rainfall activity. The selection of a 0.5 mm.hr^{-1} threshold was based on its proximity to the resolution of the tipping. Since it was expected that daytime and nighttime conditions are different, considering the presence or absence of solar radiation, we decided to separate the rain events into daytime events (occurring between 8:00 and 17:00 Local Manaus Time) and nighttime events (occurring between 20:00 and 5:00 Local Manaus Time). All composite results are presented as median values.

Between 2013 and 2020, a total of 1291 rain events were recorded. Since the collection period was different for each group of gases, the amount of to-be-studied rain events differed per group. The composite dataset utilized 647, 650, 673, and 774 rain events during the daytime and 286, 285, 291, and 264 rain events during the nighttime for CO_2 , CH_4 , CO , and O_3 , respectively. For NO and NO_2 , the data spanned the period from 2018 to 2020, but due to the intricacies associated with the measurement of NO and NO_2 , certain time intervals experienced data gaps. Consequently, these gaps impacted the composite dataset when combined with rainfall data. The composite datasets involving rainfall events were derived from 114 and 54 rain events during the day and night, respectively, for NO . Similarly, for NO_2 , the composites were constructed using 104 and 54 rain events during the day and night. In the case of Volatile Organic Compounds (VOCs), collected between November 2012 and December 2015, the composite datasets that considered rainfall events were calculated using 258 rain events during the daytime and 94 rain events during the nighttime. The various gases, their corresponding data collection periods, and the influence of rainfall events have contributed to a complex dataset that captures the dynamics of atmospheric constituents over the Central Amazon.



2 Results and Discussion

185 The analysis is based on a composite of several gas concentration profiles covering GHGs and reactive gases, including selected
BVOC during rainfall events, as similarly studied for aerosol in the Amazon (Machado et al., 2021). This comprehensive
examination covers both daytime and nighttime periods. To enhance the discussion and interpretation, we commence the
analysis by examining the median profiles for each gas species during day and night. These profiles were computed inside the
4-hour time window, centered at the moment of the maximum rain rate. Subsequently, we will delve into the analysis of ^{222}Rn
190 activity, utilized as a tracer for assessing surface-atmosphere mixing, alongside examining pertinent weather variables during
precipitation events.

2.1 Day and night mean profile of gas concentration during rainfall events

The gas profiles depicted in Figure 1 serve as the baseline for the composite analysis, emphasizing variations in the profiles
leading around (4-hour window) of the precipitation events. Composites were derived by calculating deviations from the
median profile within a 4-hour window, covering 2 hours before and 2 hours after the peak rain rate. The profiles presented in
195 Figure 1 represent the basis for calculating gas concentration anomalies in the composites. The CO_2 profile exhibits distinct
patterns, characterized by elevated concentrations at night, a gradual reduction within the canopy during the day, and a relatively
constant concentration above the canopy. During the nocturnal hours, the vertical gradient of the concentration decreases
steadily. These profiles clearly show the nighttime source of CO_2 within the canopy. Similarly, CO demonstrates analogous
200 patterns, with its vertical distribution exhibiting similarities between day and night. In contrast, CH_4 displays higher daytime
concentrations compared to nighttime levels, and its vertical variability remains minimal, typically less than 4 ppb. During
daytime, the peak concentration occurs near the surface, while it occurs above the canopy level at night. These profiles provide
insights into the different vertical dynamics of greenhouse gases with strong sources and sinks, like CO_2 , and weak or absent
local sources like CH_4 .

205 The O_3 profile follows a similar diurnal pattern, with higher concentrations during the daytime and an increase in concentration
with height. O_3 concentration and vertical variation are nearly identical during the day and night. O_3 varies from surface to
79 m by 7 ppb during the day and 6 ppb at night. This day/night contrast becomes more pronounced above the canopy level.
These profiles illustrate how ozone-rich air infiltrates the canopy during rainfall events, contributing to its complexity. The
faster decrease in O_3 concentrations within the canopy primarily results from the interactions between BVOCs and O_3 and
210 reaction with the vegetation, as highlighted by (Freire et al., 2017). Nevertheless, during instances of rain and, consequently,
downdrafts, a surge in turbulence occurs within the canopy, leading to the upward movement of air from the top to the bottom.
This atmospheric transport mechanism contributes to an augmentation in O_3 concentrations within the canopy, as elucidated
by Mendonça et al. (2023). Conversely, the concentration of NO remains primarily confined within the canopy, with marginal
differences between day and night. However, a distinction arises above the canopy, where nighttime concentrations increase
215 faster. This characteristic delineates the interplay of ground-level production and consumption processes within and above the



canopy, influenced by the dynamics of the nocturnal boundary layer and its impact on nighttime concentration levels. NO₂ exhibits the most distinct day-night contrast in its characteristics. At night, its concentration remains relatively homogeneous, while during the day, there is an exponential decrease in concentration from within the canopy to higher altitudes. Additionally, nighttime concentrations above the canopy are higher, indicating production and accumulation within the canopy and consumption within and above during daylight hours.

Isoprene and monoterpenes display similar behavior, with their primary source at the canopy's top. Their concentrations decrease both above and below the canopy. During nighttime, isoprene exhibits minimal variation in concentration with height, showing a nearly uniform distribution, with a gradual increase with altitude. In contrast, monoterpenes accumulate within the canopy during nighttime, with a particular release during rainfall events. Although its concentration is lower than daytime levels, its vertical distribution remains consistent. The monoterpene production could be influenced by mechanical turbulence within the vegetation, especially during rainfall events, and modulated by the air temperature.

2.2 Vertical mixing and Environmental characteristics during rainfall events

Changes in gas concentration during rainfall events could be modulated by an ensemble of effects, from the vertical advection of free troposphere air, changes in surface fluxes, changes in the cloud cover inducing a reduction in solar radiation reaching the canopy, changes in temperature, the wash-out effect by the rain, among others processes [Pedruzo-Bagazgoitia et al. \(2023\)](#). In order to evaluate the effect and dynamics of the soil fluxes, we used a proxy value based on atmospheric ²²²Rn activity concentration measurements. Of course, this proxy only applies to gases that are co-emitted with ²²²Rn from the soil, such as CO₂, NO and possibly CH₄ after a rain event. The relative humidity threshold (<95%) employed in the data analysis considerably reduced the sample size; for the day events, the composite had 109 cases, and for the night, 23 cases. Figure 2 shows how ²²²Rn varies before the maximum rainfall event during the day and during the night, measured at 80 m height above the ground. During the day, the ²²²Rn activity concentration is nearly constant 2 hours before the maximum rain rate. There is a slight decrease half an hour before the moment of maximum rainfall, which is likely due to the effect of the onset of precipitation, causing washout and radioactive imbalance thereafter. On the other hand, during nighttime, radon concentrations peak one hour before the maximum rain intensity, followed by a slight drop in activity concentration and also half an hour before the moment of maximum rainfall, probably due to the same wash-out effect. We should observe a large variability during the night due to the small sample. However, we tested the behavior separately for only 2019 and 2020, and the pattern of maximum activity concentration before maximum rainfall is consistent between the two years. This analysis suggests that preceding rain events, there is a nearly constant surface flow during the day and an increase in surface flows at night. These features will be discussed in detail in the upcoming subsections. The increase in radon activity concentrations is more pronounced during nighttime, possibly linked to atmospheric stability leading to the accumulation of trace gases that have a local source. For further evaluation of the ²²²Rn behavior with other gases (CO₂, CO, CH₄) see Supplement Figures ?? showing the behavior

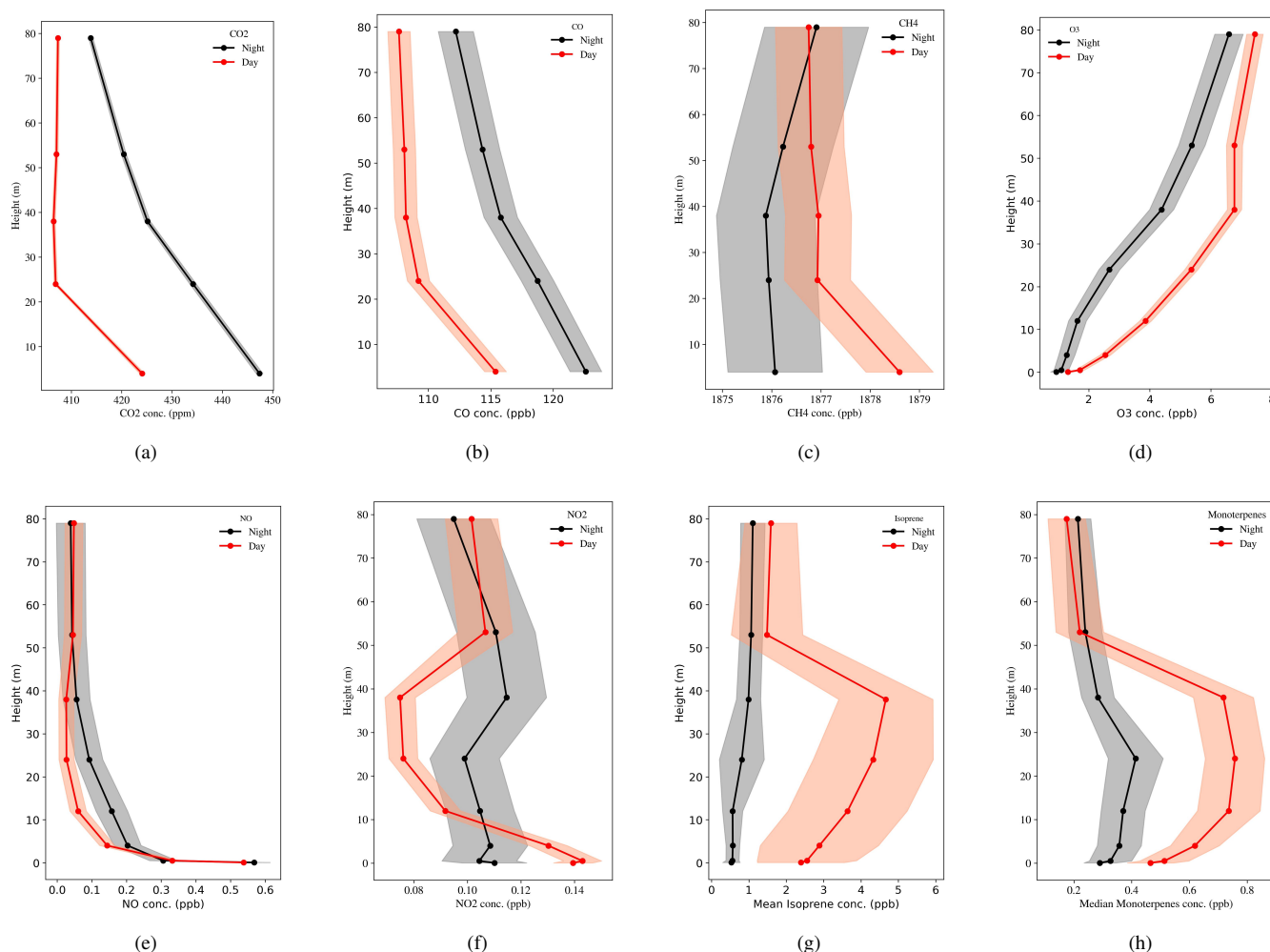


Figure 1. Vertical profiles of median concentrations and 99% confidence interval, for CO₂, CO, CH₄, NO, NO₂, isoprene, and monoterpenes during the day (red) and night (black), for all rain-events. The dataset to compute the median spans a two-hour window before and after the peak rain rate. The total number of rain events for each gas is detailed in the Data Analysis section.

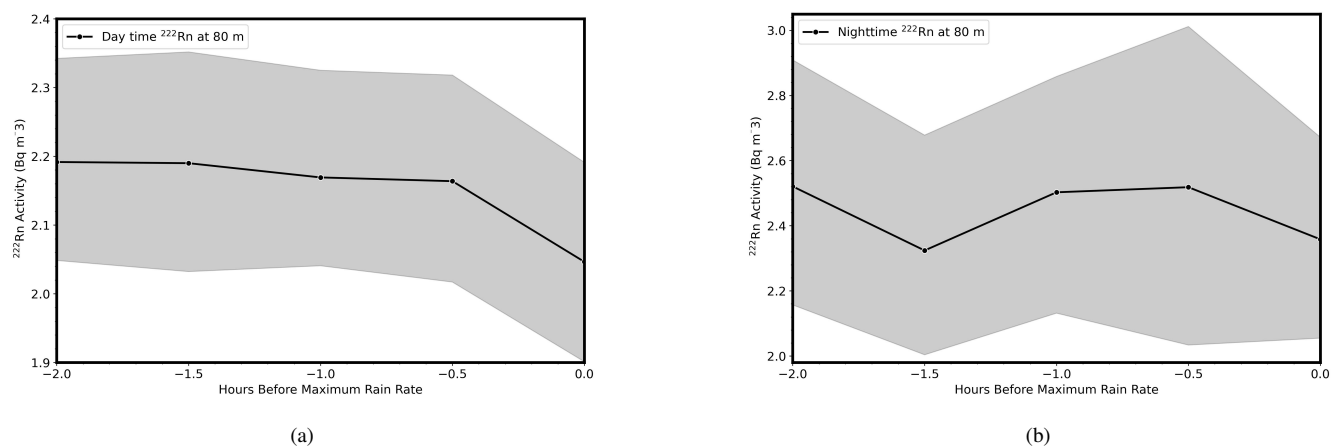


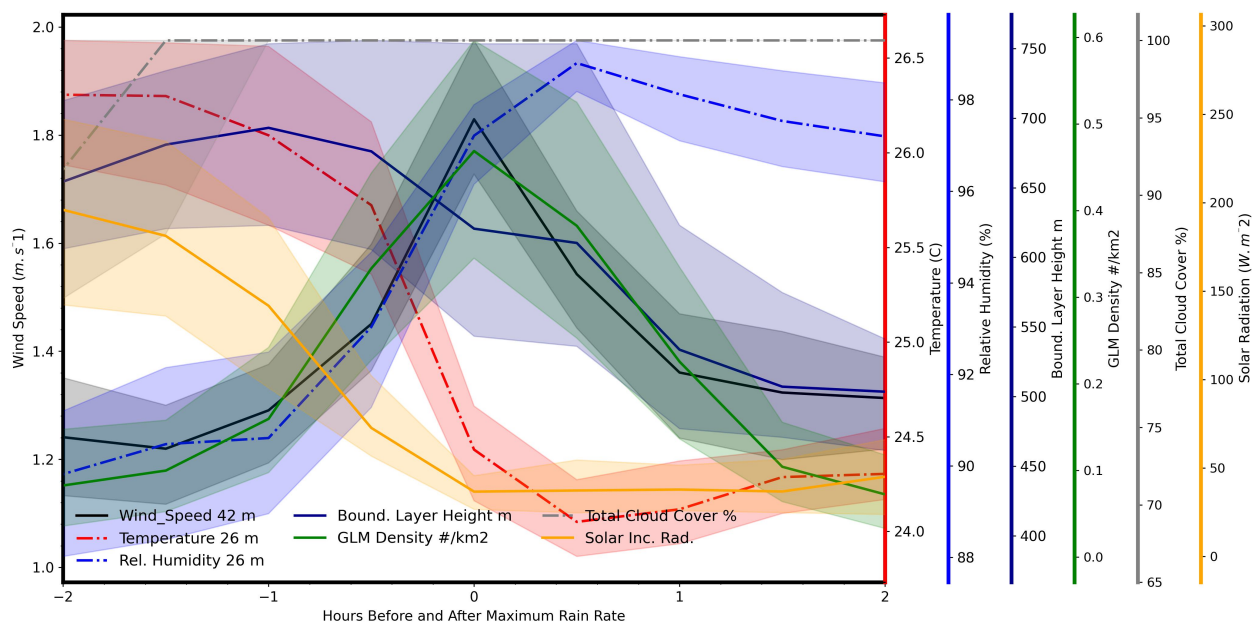
Figure 2. Composite of ^{222}Rn concentrations at 80 m above ground during day (a), and night (b), from two hours before to the time of the maximum rain rate. After the rain, part of the atmospheric radon progeny could have been lost due to scavenging effects and to avoid this imprecision ^{222}Rn activity concentrations are not reported after maximum rain rate. A rainfall event was considered as an event inside the 4-hour window with at least one moment with a rain rate larger than $0.5 \text{ mm}\cdot\text{hr}^{-1}$. The data used covers rain events from January 2019 to December 2020. Values are presented as the median values, and the gray shading is the 95% confidence interval.

side by side, with normalized variation based in standard variation. These Figures will be discussed during the analysis of each of these gases in the next session.

Figure 3 illustrates the temporal variations in several key meteorological parameters, including temperature, relative humidity, wind speed, solar radiation, boundary layer height, and lightning events within a 4-hour window surrounding the time of maximum rain rate. Temperature exhibits a decreasing trend from 1 hour prior to the peak rainfall, reaching its lowest point approximately 30 minutes after the maximum rainfall intensity. Conversely, relative humidity experiences a steady increase, with the highest humidity levels occurring about 30 minutes after the peak rainfall. Wind speed attains its maximum value at the time of the highest rainfall rate, while total cloud cover shows an overcast situation 1.5 hours before the maximum rain rate, and solar radiation registers its lowest value concurrently with the maximum rain rate. Boundary layer height initiates a decline around 30 minutes before the maximum rainfall, indicating a notable influence of precipitation on the atmospheric boundary layer. Furthermore, lightning events (hereafter called GLM events) reach their maximum at the same time. Throughout the text, we will examine and discuss these observed features. Calculations were done considering day and night together.

2.3 Greenhouse gases, Carbon Monoxide and rainfall events

To effectively illustrate the variations in the gas profiles before and during precipitation events, the calculations were performed as deviations from the average profile within 4-hour windows, spanning 2 hours before and 2 hours after the peak rain rate.



(a)

Figure 3. Composite of weather variables for two hours before the maximum rain rate to two hours after air temperature at 26 m, relative humidity at 26 m, wind speed at 42 m, solar radiation, GLM lighting events, boundary layer height, and cloud cover. A rainfall event was considered as an event inside the 4-hour window with at least one moment with a rain rate larger than 0.5 mm.hr^{-1} . Values are presented as the median values, except for the GLM lighting, because lighting events are not frequent and the median value is zero, so we used the mean for GLM lighting. The shaded bands around the median or mean values correspond to the 95% confidence interval.

To enhance visual clarity, the figures represent the deviation inside the 4-hour window, centered in the moment of maximum rain rate, and employing distinct scales to accentuate pre- and post-rain contrasts. This analytical approach is of significant importance due to its capacity to unveil gas concentration variability caused by rainfall. The accurate replication of these patterns by models is crucial for the precise computation of the gas budget and life cycle.

A composite study of the gas profile measurements, conducted both during the day and night and inside and above the canopy, provides a comprehensive opportunity to investigate the impact of rainfall on greenhouse gases (GHGs), specifically CO_2 and CH_4 . Figure 4 depicts the diurnal and nocturnal evolution of the deviation from the median profile, presented in the precedent section, for CO_2 , CO , and CH_4 concentration profiles within a two-hour window before and after the peak of rainfall events.

The majority of gas concentrations exhibit a decline concurrent with precipitation. The CO_2 profile varies between the surface and above the canopy at 79m, before and after the rain event, around 1.8 ppm during the day to 3.3 ppm at night (total range of variation). While CO_2 concentration shows limited sensitivity to rain, particularly near the surface during the day, the influence is more pronounced at night, manifesting a significant reduction in concentrations both within (day and night) and just above the canopy (night). This data underscores the variable response of CO_2 concentrations to rainfall, emphasizing its more



275 prominent role in nocturnal conditions, possibly due to the enhanced mixing conditions associated with rainfall are having a relatively larger impact on the nighttime CO₂ concentration buildup than on the relatively well-mixed daytime CO₂ profile. CO₂ concentrations, possibly affected by local sinks and sources (vegetation and soil), increased before and decreased after the maximum rain rate inside the canopy and during the day and at night. Higher concentrations near the ground and lower ones at the canopy height point at sources close to the forest floor, such as soil and lower canopy respiration, and a stronger vegetational
280 photosynthetic sink at the higher heights. The rain event seems to mask CO₂ accumulation near the ground, whereas it seems to spark an increase in CO₂ concentrations at higher heights.

The decrease of CO₂ concentration within the canopy after the rainfall is directly linked to the simultaneous increase in humidity and cloud cover and decrease in temperature. These environmental conditions suppress both soil and tree CO₂ exchange as well as surface flux and reduce photosynthesis. Another possible reason could be associated with an increase in mixing within
285 the canopy, destroying the stable layer within the canopy by mixing free tropospheric air into the canopy. It is possible that these two effects contribute to the reduction in CO₂ concentration after the rain event; however, the importance of each of these effects could not be quantified with the current data. Above the canopy, this decline is most likely attributed to the transport of free tropospheric air with low CO₂ into the boundary layer. This phenomenon becomes less important, presumably due to a reduction of free-air injection by the formation of the nocturnal boundary layer and strengthened by accumulation driven by
290 soil and plant respiration.

During the night before the rain event, there is a clear increase in concentration at 70 m according to the radon surface flux proxy (see Supplementary Figures ??). It is possible that the nocturnal production of CO₂ combined with the turbulent fluxes associated with the gust fronts of the rain events produces this increase in concentration above the canopy. The rain event itself leads to a turbulent mixing of air from above down to the ground resulting in a strong decrease of CO₂ concentration.

295 The evaluation of CO concentrations around rain events (Figure 4c,d) shows a similar picture as observed for CO₂, though with some small differences. Under daylight conditions and before the rain event, CO profiles exhibit a strong source near the ground and show lower concentrations near the canopy. Thus, there is likely a source of CO near the forest floor (van Asperen et al., 2023). In global CO inventories, the biosphere is regarded to act as both a source and a sink, but large uncertainties remain about the strength of individual sources. CO emissions are usually associated with abiotic degradation of organic matter, in the
300 form of photodegradation (Guenther, 2002; Seiler and Conrad, 1987; Schade et al., 1999; Tarr et al., 1995; Derendorp et al., 2011) as well as thermal degradation (Yonemura et al., 1999; Lee et al., 2012; van Asperen et al., 2015). Living plants have also been reported to show CO emissions, but are expected to be minimal compared to senescent plant material (Derendorp et al., 2011; Schade et al., 1999; Tarr et al., 1995). Besides soil CO emissions, soil CO consumption cannot be excluded: soil microorganisms are known to oxidize CO to CO₂, a process, among others, dependent on available oxygen (soil diffusivity)
305 and temperature King and Hungria (2002). As underlined by Liu et al. (2018), the balance between soil CO uptake, and soil CO emission is not well understood, especially in the tropics.



During the day, the overall picture changes completely with rainfall, shifting from a strong vertical gradient towards a relatively well-mixed layer from the ground to 79 m. However, after the maximum rain rate, a further decrease in CO concentrations near the forest floor is observed, possibly pointing to decreased CO emission or increased CO uptake. The picture at night shows more homogeneous mixing from ground to 80 m but with still slightly higher CO concentrations close to the forest floor. Just as during the day, the precipitation event causes an inversion of the profile, indicating a change in the ratio between CO uptake and emissions processes with the same transport phenomena discussed for CO₂. Above the canopy, during the night, at 79 m, there is a very slight increase in the concentration of CO before the maximum rain rate (see Supplementary Figures), related to the increase in turbulent surface fluxes as observed for CO₂, but less clear for a probably smaller nocturnal source of CO, comparable to that of CO₂ (see Supplementary Figures).

CH₄ (Figure 4e, f), in contrast to the other gases, displays notably less stratification, with variations spanning from the surface to 79 meters, amounting to less than 2 ppb throughout both day and night periods. Although this variance might seem minor, a discernible pattern emerges: the highest concentrations are at the surface during the day, while during the night, they are more prevalent in higher altitudes. This daytime behavior can be attributed to weak sources of CH₄ production, primarily stemming from microbial anaerobic decomposition processes, depending on temperature and soil humidity, occurring mainly near the ground. As temperatures decrease during nighttime, CH₄ production wanes, possibly leading to the observed shift in concentration peaks toward upper levels. Assuming the inlet at 79-m height is within the nocturnal boundary layer, the nocturnal maxima can be explained by the processes described in Botía et al. (2020), but if the inlet height is above the nocturnal boundary layer and inside the residual layer, the CH₄ peak could be associated with the concentration of the previous afternoon. The impact of rain on CH₄ concentration is comparably modest compared to other gases, resulting in an alteration of approximately 6 ppb. As CO₂ and CO, CH₄ exhibits a time trend with rainfall with minimum concentration two hours subsequent to the peak rainfall intensity. The supplementary information presented in Figure ?? shows a practically unchanged concentration of CH₄ during the night before the rain events, which indicates that although there are turbulent fluxes at the surface, the concentration is not affected above the canopy, probably due to the absence of sources at that time.

Generally, the greenhouse gas concentrations (CO₂, CO, and CH₄) revealed a similar pattern during day and night and, overall, there is a noticeable declining trend in their concentrations before reaching the peak of the rain intensity. This pattern implies that atmospheric transport plays a pivotal role in regulating the levels of trace gases, as evidenced by the concurrent rise in wind speed and boundary layer height, as depicted in Figure 3, leading up to the maximum rain rate.

During nighttime, the influence of atmospheric transport on CO and CH₄ concentrations before reaching the maximum rain rate is less pronounced compared to daytime. The concentrations of these gases exhibit only minor variability until the point of maximum rain intensity. However, the situation differs for CO₂, which displays a significant peak roughly equivalent to one standard deviation, occurring half an hour before the maximum precipitation intensity. This notable peak could be indicative of a localized source of CO₂ at canopy height and the surface turbulent flux that impacts the concentration at the 79-meter level.



340 The effect of air transport from the free troposphere to the canopy should be the same for all the gases, as it is related to the
amount of air exchanged. However, the source-sink patterns of the three gases in terms of time and location within the canopy
differ, implying the pattern observed in these compounds. The data used in this study does not allow the effects of transport to
be completely separated from the effects of sources and sinks. The composite highlights distinct patterns associated with the
rain events in the gases presented here. For CO₂, the strong vertical gradient for night and day with high mole fractions within
the canopy suggests a local production of the gas and poor CO₂ gas concentration transported from the free atmosphere. In
345 contrast, CO profiles could be affected by vertical transport, whereas the minimal vertical gradient of CH₄ could indicate an
almost balanced local production/sink relationship.

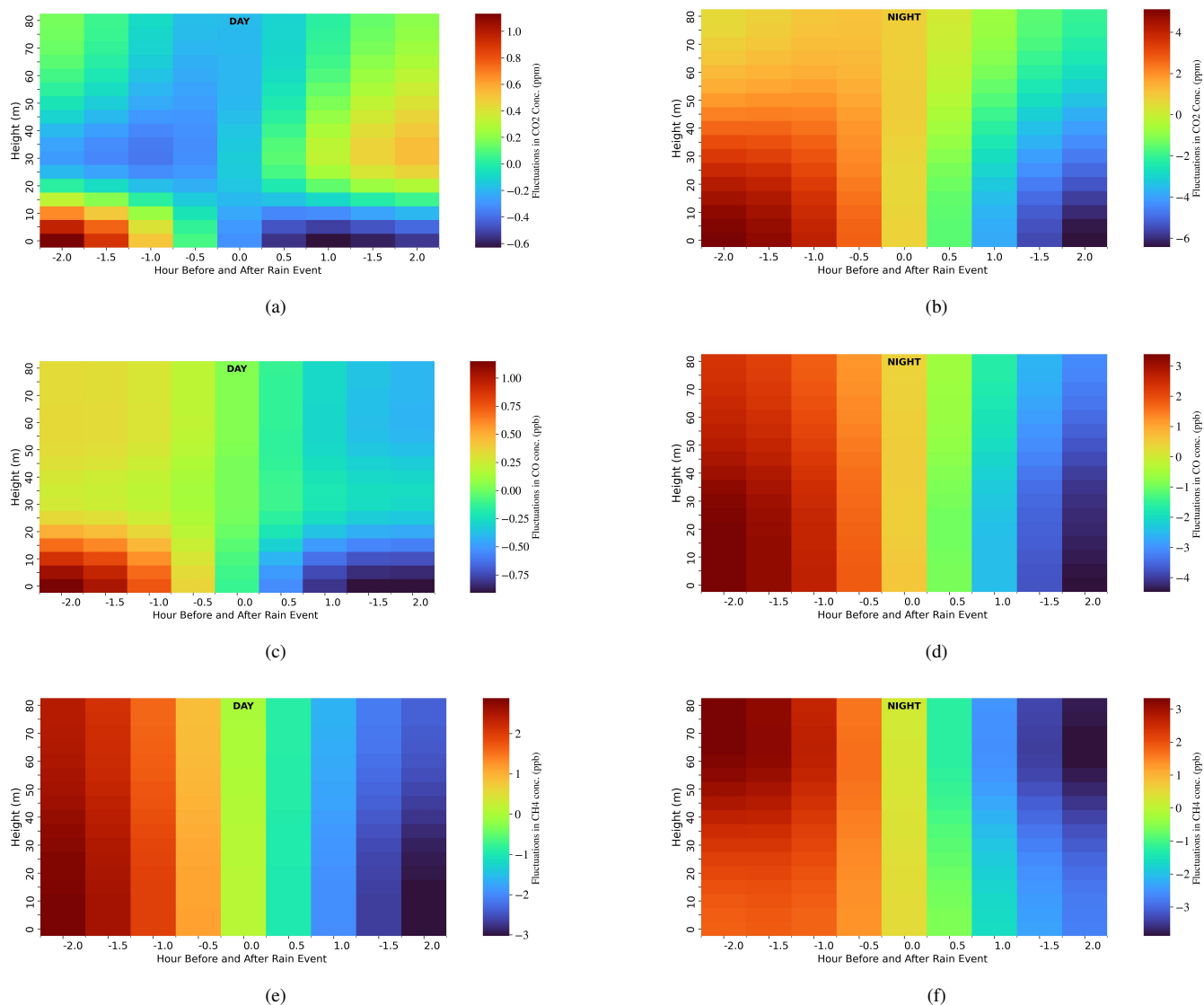


Figure 4. Composite of CO₂ during the day (a), and night (b), CO during the day (c) and during the night (d), and CH₄ during the day (e) and during the night (f), for two hours before the maximum rain rate to two hours after. Please note that the color bar scale is different between each figure. A rainfall event was considered as an event with at least one case with a rain rate larger than $0.5 \text{ mm}\cdot\text{hr}^{-1}$. Calculation was done for all cases from January 2013 to December 2020. Values are presented as the deviation from median composite values.



2.4 Reactive gases and rainfall events

Figure 5 shows the evolution of O_3 , NO, and NO_2 concentration profiles during the day (a,c,e) and during the night (b,d,f), two hours before and after the maximum rainfall. 5 (a,b,) shows O_3 concentration increasing during precipitation events, as
350 observed by Wang et al. (2016); Gerken et al. (2016); Sigler et al. (2002). A considerable increase is driven by a downdraft reaching the ground. This injection of ozone-rich air from the upper levels reaches a maximum of about one hour after rainfall. The O_3 increase within the canopy can be attributed to the injection of high levels of O_3 concentration in the upper troposphere. O_3 concentration is related to atmospheric chemistry, cloud dynamic transport, and cloud electrification (Brune et al., 2021; Williams et al., 2002), as indicated by a maximum lightning activity at this time. Of special interest is the less striking vari-
355 ation of the O_3 concentration just around and above the canopy during the day, before and after rainfall. This result indicates deposition, decomposition, or uptake by vegetation. This kind of sink masks the variation as affected by the rain event. As this level represents the main source for isoprene and monoterpenes, mainly during the day, a reaction with these VOC species may play a crucial role. The NO/ NO_2 dynamics within the precipitation event seems to reflect this complex series of reactions near the surface and above the canopy, starting with soil NO emission and accumulation affected by O_3 , transport processes and
360 chemical reactions, resulting in the production of NO_2 . This general view is supported by several reports based on chamber and field studies in Rondonia (Rummel et al., 2002; Gut et al., 2002; Kesselmeier et al., 2002; Chaparro-Suarez et al., 2011; Bell et al., 2022; Zhao et al., 2021) indicating the oxidative regime as to be governed by O_3 and affecting several trace gases. These studies contribute to our understanding of the within-forest oxidative capacity reflected by VOC oxidation products, such as formaldehyde, as observed under daytime conditions near the forest surface (Rottenberger et al., 2004). During the day, the
365 rainfall event leads to an opposite behavior between NO_2 and NO; the former is increased during rainfall, and NO decreases after the rainfall. NO variation with rainfall mostly occurs within the canopy. During the night, the effect is also observed above the canopy, probably due to the small height of the nocturnal boundary layer. For NO_2 , the variation with rain is highest just above the canopy. However, during the night, a different pattern emerges, showing the importance of solar radiation in the daily photo-chemical reaction. During the night, the highest variations of NO_2 concentration primarily occur around the canopy top.
370 This can be understood as caused by vegetation's missing NO_2 uptake. Under daylight, with open stomata, the plant leaves are effectively taking up NO_2 from the air, whereas stomata are closed in the dark, and the sink strength decreases to negligible (Chaparro-Suarez et al., 2011). The rainfall events at night show NO_2 being washed out from the air above the canopy, with the strongest loss at the canopy top. Interestingly, a small positive variation remains near the ground after the rainfall. However, this potential source remains unclear as the rain does not activate any soil NO source to produce NO_2 . Nevertheless, the behavior
375 of NO fluctuations within the forest show an expected picture of accumulation before and decreasing concentration after rain. Although the absolute difference with rain events is small, it corresponds to about 10% variation.

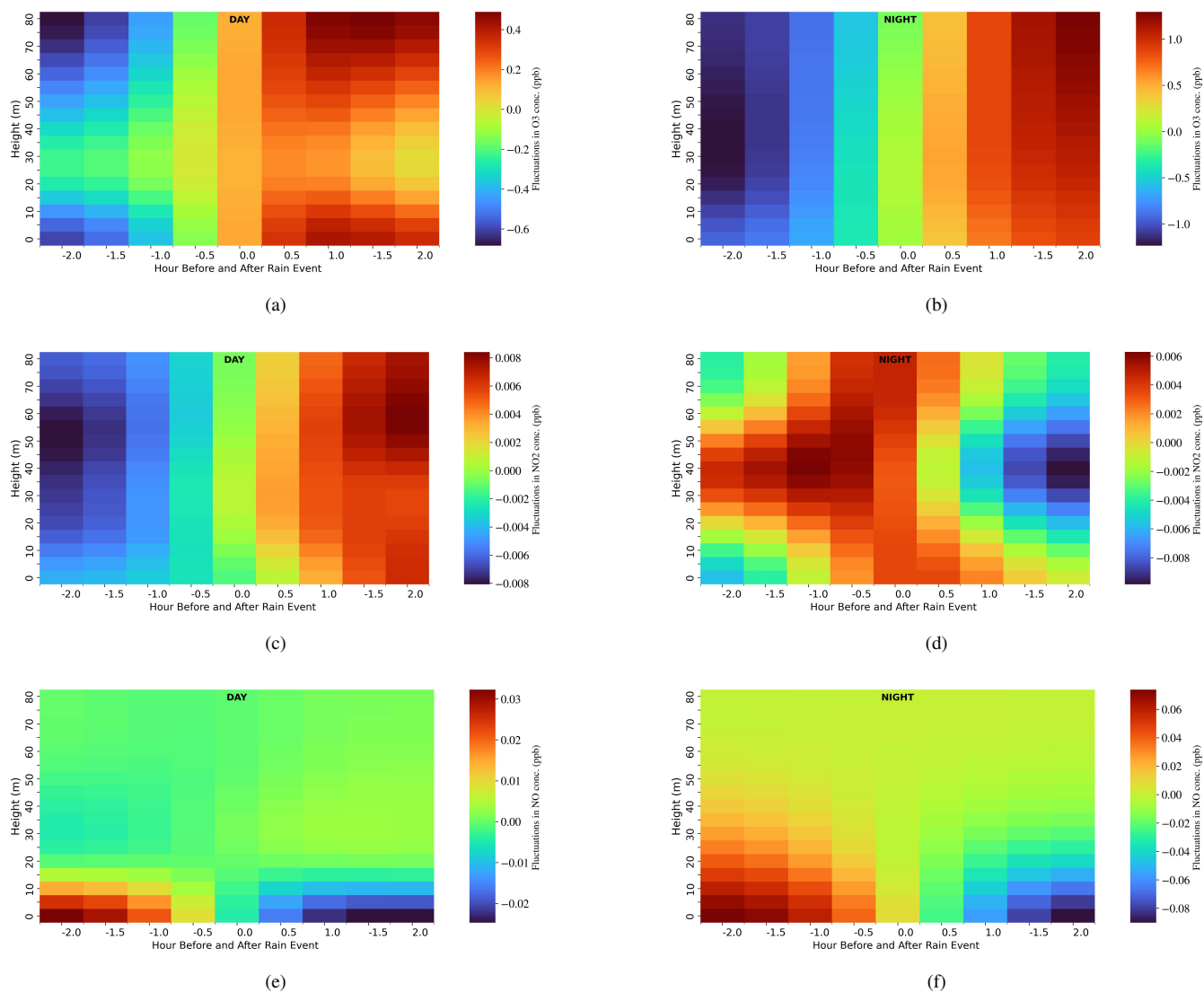


Figure 5. Composite of O₃ during the day (a), and night (b), NO₂ during the day (c) and during the night (d), and NO during the day (e) and during the night (f), for two hours before the maximum rain rate to two hours after. A rainfall event was considered as an event inside the 4-hour window with at least one moment with a rain rate larger than 0.5 mm.hr⁻¹. Calculation was done for all cases from January 2013 to December 2020. Values are presented as the deviation from median composite values.



2.5 Volatile Organic Compounds and rainfall events

Figure 6 shows the evolution of isoprene and monoterpenes concentration profiles during the day (a,c) and during the night (b,d) two hours before and after the maximum rainfall. The depletion of biogenic VOC under these conditions can generally be related to oxidative atmospheric chemistry leading to secondary organic aerosol. The most important biogenic non-methane VOCs, isoprene and monoterpenes, have their maximum concentration increase about two hours before the rain peak during the day related to canopy release and upward transport, driven by the meteorological conditions before rainfall, mostly with high air temperatures and intensive solar radiation favoring the biogenic synthesis of isoprene and monoterpenes. As soon as rain starts, the temperature and solar irradiance drop rapidly, directly affecting biogenic trace gas production. Subsequently, during this time (daytime), the concentrations continue to be lower than before the rain event. This basic behavior is observed at all levels and is comparable to the observations of isoprene after rain events reported in (Pfannerstill et al., 2021). The clear loss of isoprene and monoterpene emission causes a sharp concentration decrease above the canopy. This drop indicates a set of decomposition pathways, deposition processes, and consumption inside the canopy. Under night conditions, a constant decrease of isoprene is observed before the rain event, followed by a slight increase of isoprene near the ground under rainfall, and it even affects higher heights in the course of time after rainfall. This observation of an increase in isoprene concentration during the night looks puzzling, but only at first view. We have to regard the biosynthesis of this compound. Plants produce isoprene with chloroplasts (see (Lichtenthaler, 1999)) for an overview. But the chloroplastic pathway is of bacterial origin (Rohmer et al., 1993, 1996) imported by endosymbiosis, a relic of bacterial pathways through the evolution of plastids, obviously. More recently, bacterial isoprene synthesis was confirmed and described as a general issue of the bacterial genome (Sivy et al., 2002; Rudolf et al., 2021). Thus, we understand the isoprene increase and accumulation near the ground under night conditions as a result of a light-independent microbial production of this compound, which becomes visible under the applied composite description around rainfall. Furthermore, this pathway might also contribute to further isoprenoid accumulation, i.e., that of monoterpenes. Monoterpenes have a lower concentration during the night, but in contrast to isoprene, the pattern caused by the rain event shows a clear accumulation before the rainfall peaks. This maximum is located at a lower altitude above the forest canopy than during the day. Obviously, there is a source within the lower layers of the forest. We may only speculate about such potential sources, for example, plant tissues with stored monoterpenes physically affected by raindrops, such as glands or hairs, or mechanical turbulence caused by the gust front associated with the convective process.

3 Conclusions

The combination of rainfall data with gas profiles collected at the ATTO site over several years provides insight into the trace gas variability during rainfall events. This analysis provides a quantitative description of greenhouse gases, reactive inorganic and volatile organic compounds at different heights within and above the canopy and being affected by meteorological events.

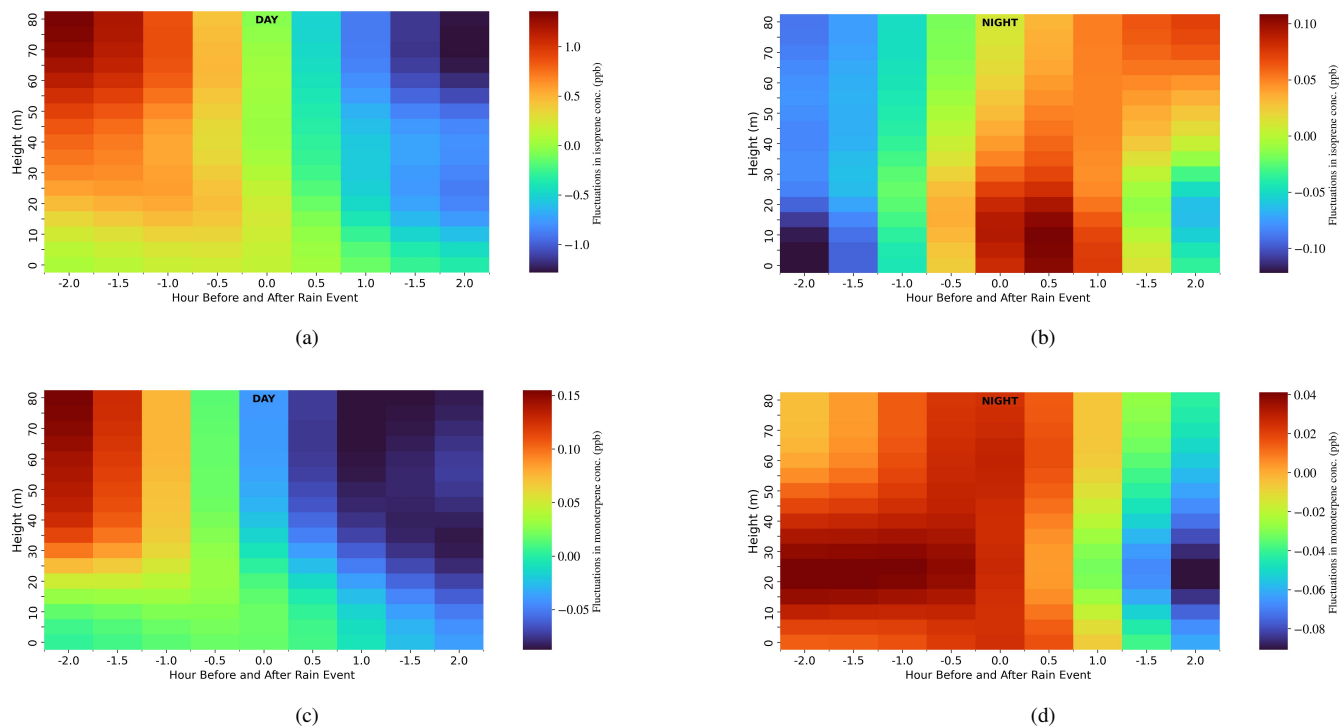


Figure 6. Composite of isoprene during the day (a) and night (b), monoterpenes during the day (c) and during the night (d), for two hours before the maximum rain rate to two hours after. A rainfall event was considered inside the 4-hour window with at least one moment with a rain rate larger than $0.5 \text{ mm}\cdot\text{hr}^{-1}$. Calculation was done for all cases from January 2012 to December 2015. Values are presented as the deviation from median composite values.

The average profile for each gas computed based on the median-composite 2 hours before to 2 hours after a rainfall event during day and night clarifies several aspects of the gas behavior within and above the canopy. BVOC, O_3 and CH_4 present larger concentrations during the day, and CO_2 , CO , and NO have maximum concentration during the night, NO_2 has a mixed
410 behavior, with a larger concentration near the ground during the day and above the canopy concentration is larger during the night. For all species, except for NO_2 , the nighttime profile is more homogeneous as a result of the shallow nocturnal boundary layer. These profiles indicate the source of each gas, such as the canopy top for VOC, respired from leaves and stems and ground surface for CO_2 , and ground surface for CO , and CH_4 and free-atmosphere for O_3 .

The ^{222}Rn is used as a surface flow tracer before rain events to complement the data analysis. There is a difference between day
415 and night. During the day, the activity of ^{222}Rn remains practically unchanged for two hours before the moment of maximum rainfall, while at night there is an increase in the concentration of radon activity one hour before the moment of maximum rainfall. This indicates a greater impact on the soil surface flux during the nocturnal rain event.



Composite analysis of the gas concentration before and after rainfall, during the day and night, gives insight into the complex relationship between trace gas variability and precipitation. Entrainment from above may affect the mixing above and within the forest. This analysis improves our understanding of trace gas sinks and sources. CO₂, CO, and CH₄ decrease with rain, probably related to the clean air injected into the boundary layer from the upper levels. CO₂ and monoxide are more stratified with height than CH₄. CO has a sharper change with rainfall than CO₂. CH₄ changes are less significant than CO₂. O₃ concentration increases during precipitation events. The patterns variability of the NO_x family in time and space is closely related to the contributing sink and source processes. As discussed above, a series of potential interactions exist between soil, atmosphere, and plants inside the canopy. Biogenic VOCs, such as isoprene and monoterpenes, change with the rainfall affected by light (production) and physical transport. The NO-NO₂ emission and reaction chain becomes visible with regard to soil emission of NO, resulting in an accumulation at night or oxidation to NO₂ and release from the forest during the day. Furthermore, rainfall can activate trace gases (NO) burst from soil or VOCs from plant storage tissues. Thus, this composite analysis helps to understand sources and sinks of trace gases within a forest ecosystem.

Data availability. All data used in the study will be available at Edmond repository, with open access.

Author contributions. Conceptualization: LATM, CP

Data curation: HVA, SPJ, JL, AYS, VIDV, SK, DW, SW, IL

Funding acquisition and administration: UP, PA, JL, CAQ, CP, ST, IL

Methodology: LATM

Writing original draft: LATM, JK, SB

Writing review & editing: All authors

Competing interests. The contact author has declared that none of the authors has any competing interests

Acknowledgements. This research has been supported by the Max Planck Society, the FAPESP grant 2022/07974-0, and the Bundesministerium für Bildung und Forschung (BMBF contracts 01LB1001A, 01LK1602B, 01LK1602C and 01LK2101B). For the operation of the ATTO site, we acknowledge the support of the Max Planck Society, the German Federal Ministry of Education and Research, and the Brazilian Ministério da Ciência, Tecnologia e Inovação as well as the Amazon State University (UEA), FAPEAM, LBA/INPA, and SDS/CEUC/RDS-Uatumã. We would like to especially thank all the people involved in the technical, logistical and scientific support of the ATTO project, in particular Reiner Ditz, Hermes Braga Xavier, Nagib Alberto de Castro Souza, Adir Vasconcelos Brandão, Valmir Ferreira de Lima, Antonio Huxley Melo do Nascimento, Amauri Rodrigues Perreira, Wallace Rabelo Costa, André Luiz Matos, Davirley Gomes

<https://doi.org/10.5194/egusphere-2023-2901>

Preprint. Discussion started: 23 January 2024

© Author(s) 2024. CC BY 4.0 License.



- 445 Silva, Fábio Jorge, Thomas Disper, Torsten Helmer, Steffen Schmidt, Uwe Schultz, Karl Kübler, Olaf Kolle, Martin Hertel, Kerstin Hippler, Fábio Jorge, Björn Nillius, Thomas Klimach, Delano Campos, Juarez Viegas, Sipko Bulthuis, Fernando Goncalves Morais, Roberta Pereira de Souza, Bruno Takeshi and Francisco Alcinei.



References

- 450 Andreae, M. O., Acevedo, O. C., Araújo, A., Artaxo, P., Barbosa, C. G., Barbosa, H. M., Brito, J., Carbone, S., Chi, X., Cintra, B. B., Da Silva, N. F., Dias, N. L., Dias-Júnior, C. Q., Ditas, F., Ditz, R., Godoi, A. F., Godoi, R. H., Heimann, M., Hoffmann, T., Kesselmeier, J., Könemann, T., Krüger, M. L., Lavric, J. V., Manzi, A. O., Lopes, A. P., Martins, D. L., Mikhailov, E. F., Moran-Zuloaga, D., Nelson, B. W., Nölscher, A. C., Santos Nogueira, D., Piedade, M. T., Pöhlker, C., Pöschl, U., Quesada, C. A., Rizzo, L. V., Ro, C. U., Ruckteschler, N., Sá, L. D., De Oliveira Sá, M., Sales, C. B., Dos Santos, R. M., Saturno, J., Schöngart, J., Sörgel, M., De Souza, C. M.,
- 455 De Souza, R. A., Su, H., Targhetta, N., Tóta, J., Trebs, I., Trumbore, S., Van Eijck, A., Walter, D., Wang, Z., Weber, B., Williams, J., Winderlich, J., Wittmann, F., Wolff, S., and Yanez-Serrano, A. M.: The Amazon Tall Tower Observatory (ATTO): Overview of pilot measurements on ecosystem ecology, meteorology, trace gases, and aerosols, *Atmospheric Chemistry and Physics*, 15, 10 723–10 776, <https://doi.org/10.5194/acp-15-10723-2015>, 2015.
- Bell, D. M., Wu, C., Bertrand, A., Graham, E., Schoonbaert, J., Giannoukos, S., Baltensperger, U., Prevot, A. S. H., Riipinen, I., El Haddad, I., and Mohr, C.: Particle-phase processing of α -pinene NO_3 secondary organic aerosol in the dark, *Atmospheric Chemistry and Physics*, 22, 13 167–13 182, <https://doi.org/10.5194/acp-22-13167-2022>, 2022.
- 460 Bertrand, G., Celle-Jeanton, H., Laj, P., Rangognio, J., and Chazot, G.: Rainfall chemistry: long range transport versus below cloud scavenging. A two-year study at an inland station (Opme, France), *Journal of Atmospheric Chemistry*, 60, 253–271, <https://doi.org/10.1007/s10874-009-9120-y>, 2008.
- 465 Betts, A. K., Gatti, L. V., Cordova, A. M., Silva Dias, M. A. F., and Fuentes, J. D.: Transport of ozone to the surface by convective downdrafts at night, *Journal of Geophysical Research: Atmospheres*, 107, LBA 13–1–LBA 13–6, <https://doi.org/https://doi.org/10.1029/2000JD000158>, 2002.
- Boschat, G., Simmonds, I., Purich, A., Cowan, T., and Pezza, A. B.: On the use of composite analyses to form physical hypotheses: An example from heat wave – SST associations, *Scientific Reports*, 6, 29 599, <https://doi.org/10.1038/srep29599>, 2016.
- 470 Botía, S., Gerbig, C., Marshall, J., Lavric, J. V., Walter, D., Pöhlker, C., Holanda, B., Fisch, G., Carioca De Araújo, A., Sá, M. O., Teixeira, P. R., Resende, A. F., Dias-Junior, C. Q., Van Asperen, H., Oliveira, P. S., Stefanello, M., and Acevedo, O. C.: Understanding nighttime methane signals at the Amazon Tall Tower Observatory (ATTO), *Atmospheric Chemistry and Physics*, 20, 6583–6606, <https://doi.org/10.5194/acp-20-6583-2020>, 2020.
- 475 Botía, S., Komiya, S., Marshall, J., Koch, T., Gałkowski, M., Lavric, J., Gomes-Alves, E., Walter, D., Fisch, G., Pinho, D. M., Nelson, B. W., Martins, G., Luijkx, I. T., Koren, G., Florentie, L., Carioca de Araújo, A., Sá, M., Andreae, M. O., Heimann, M., Peters, W., and Gerbig, C.: The CO_2 record at the Amazon Tall Tower Observatory: A new opportunity to study processes on seasonal and inter-annual scales, *Global Change Biology*, 28, 588–611, <https://doi.org/https://doi.org/10.1111/gcb.15905>, 2022.
- Bourtsoukidis, E., Behrendt, T., Yanez-Serrano, A. M., Hellén, H., Diamantopoulos, E., Catão, E., Ashworth, K., Pozzer, A., Quesada, C. A., Martins, D. L., Sá, M., Araujo, A., Brito, J., Artaxo, P., Kesselmeier, J., Lelieveld, J., and Williams, J.: Strong sesquiterpene emissions from Amazonian soils, *Nature Communications*, 9, 2226, <https://doi.org/10.1038/s41467-018-04658-y>, 2018.
- 480 Brune, W. H., McFarland, P. J., Bruning, E., Waugh, S., MacGorman, D., Miller, D. O., Jenkins, J. M., Ren, X., Mao, J., and Peischl, J.: Extreme oxidant amounts produced by lightning in storm clouds, *Science*, 372, 711–715, <https://doi.org/10.1126/science.abg0492>, 2021.



- 485 Chaparro-Suarez, I., Meixner, F., and Kesselmeier, J.: Nitrogen dioxide (NO₂) uptake by vegetation controlled by atmospheric concentrations and plant stomatal aperture, *Atmospheric Environment*, 45, 5742–5750, <https://doi.org/https://doi.org/10.1016/j.atmosenv.2011.07.021>, 2011.
- Derendorp, L., Quist, J., Holzinger, R., and Röckmann, T.: Emissions of H₂ and CO from leaf litter of *Sequoiadendron giganteum*, and their dependence on UV radiation and temperature, *Atmospheric environment*, 45, 7520–7524, 2011.
- 490 Dias-Júnior, C. Q., Carneiro, R. G., Fisch, G., D’Oliveira, F. A. F., Sörgel, M., Botía, S., Machado, L. A. T., Wolff, S., Santos, R. M. N. d., and Pöhlker, C.: Intercomparison of Planetary Boundary Layer Heights Using Remote Sensing Retrievals and ERA5 Reanalysis over Central Amazonia, *Remote Sensing*, 14, <https://doi.org/10.3390/rs14184561>, 2022.
- Franco, M. A., Ditas, F., Kremper, L. A., Machado, L. A., Andreae, M. O., Araújo, A., Barbosa, H. M., De Brito, J. F., Carbone, S., Holanda, B. A., Morais, F. G., Nascimento, J. P., Pöhlker, M. L., Rizzo, L. V., Sá, M., Saturno, J., Walter, D., Wolff, S., Pöschl, U., Artaxo, P., and Pöhlker, C.: Occurrence and growth of sub-50nm aerosol particles in the Amazonian boundary layer, *Atmospheric*
- 495 *Chemistry and Physics*, 22, 3469–3492, <https://doi.org/10.5194/acp-22-3469-2022>, 2022.
- Freire, L., Gerken, T., Ruiz-Plancarte, J., Wei, D., Fuentes, J., Katul, G., Dias, N., Acevedo, O., and Chamecki, M.: Turbulent mixing and removal of ozone within an Amazon rainforest canopy, *Journal of Geophysical Research: Atmospheres*, 122, 2791–2811, 2017.
- Gerken, T., Wei, D., Chase, R. J., Fuentes, J. D., Schumacher, C., Machado, L. A., Andreoli, R. V., Chamecki, M., Ferreira de Souza, R. A., Freire, L. S., Jardine, A. B., Manzi, A. O., Nascimento dos Santos, R. M., von Randow, C., dos Santos Costa, P., Stoy, P. C.,
- 500 Tóta, J., and Trowbridge, A. M.: Downward transport of ozone rich air and implications for atmospheric chemistry in the Amazon rainforest, *Atmospheric Environment*, 124, 64–76, <https://doi.org/https://doi.org/10.1016/j.atmosenv.2015.11.014>, 2016.
- Greenberg, J., Asensio, D., Turnipseed, A., Guenther, A., Karl, T., and Gochis, D.: Contribution of leaf and needle litter to whole ecosystem BVOC fluxes, *Atmospheric Environment*, 59, 302–311, <https://doi.org/https://doi.org/10.1016/j.atmosenv.2012.04.038>, 2012.
- Guenther, A.: The contribution of reactive carbon emissions from vegetation to the carbon balance of terrestrial ecosystems, *Chemosphere*,
- 505 49, 837–844, [https://doi.org/https://doi.org/10.1016/S0045-6535\(02\)00384-3](https://doi.org/https://doi.org/10.1016/S0045-6535(02)00384-3), 2002.
- Gut, A., Scheibe, M., Rottenberger, S., Rummel, U., Welling, M., Ammann, C., Kirkman, G. A., Kuhn, U., Meixner, F. X., Kesselmeier, J., Lehmann, B. E., Schmidt, W., Müller, E., and Piedade, M. T. F.: Exchange fluxes of NO₂ and O₃ at soil and leaf surfaces in an Amazonian rain forest, *Journal of Geophysical Research: Atmospheres*, 107, LBA 27–1–LBA 27–15, <https://doi.org/https://doi.org/10.1029/2001JD000654>, 2002.
- 510 Hirsch, A. I.: On using radon-222 and CO₂ to calculate regional-scale CO₂ fluxes, *Atmospheric Chemistry and Physics*, 7, 3737–3747, <https://doi.org/10.5194/acp-7-3737-2007>, 2007.
- Holanda, B. A., Pöhlker, M. L., Walter, D., Saturno, J., Sörgel, M., Ditas, J., Ditas, F., Schulz, C., Franco, M. A., Wang, Q., Donth, T., Artaxo, P., Barbosa, H. M. J., Borrmann, S., Braga, R., Brito, J., Cheng, Y., Dollner, M., Kaiser, J. W., Klimach, T., Knote, C., Krüger, O. O., Fütterer, D., Lavrič, J. V., Ma, N., Machado, L. A. T., Ming, J., Morais, F. G., Paulsen, H., Sauer, D., Schlager, H., Schneider,
- 515 J., Su, H., Weinzierl, B., Walser, A., Wendisch, M., Ziereis, H., Zöger, M., Pöschl, U., Andreae, M. O., and Pöhlker, C.: Influx of African biomass burning aerosol during the Amazonian dry season through layered transatlantic transport of black carbon-rich smoke, *Atmospheric Chemistry and Physics*, 20, 4757–4785, <https://doi.org/10.5194/acp-20-4757-2020>, 2020.
- Holanda, B. A., Franco, M. A., Walter, D., Artaxo, P., Carbone, S., Cheng, Y., Chowdhury, S., Ditas, F., Gysel-Beer, M., Klimach, T., Kremper, L. A., Krüger, O. O., Lavric, J. V., Lelieveld, J., Ma, C., Machado, L. A. T., Modini, R. L., Morais, F. G., Pozzer, A., Saturno, J., Su, H., Wendisch, M., Wolff, S., Pöhlker, M. L., Andreae, M. O., Pöschl, U., and Pöhlker, C.: African biomass burning affects aerosol
- 520 cycling over the Amazon, *Communications Earth & Environment*, 4, <https://doi.org/10.1038/s43247-023-00795-5>, 2023.



- Kesselmeier, J. and Staudt, M.: Biogenic Volatile Organic Compounds (VOC): An Overview on Emission, Physiology and Ecology, *Journal of Atmospheric Chemistry*, 33, 23–88, <https://doi.org/10.1023/A:1006127516791>, 1999.
- 525 Kesselmeier, J., Kuhn, U., Rottenberger, S., Biesenthal, T., Wolf, A., Schebeske, G., Andreae, M. O., Ciccioli, P., Brancaleoni, E., Frattoni, M., Oliva, S. T., Botelho, M. L., Silva, C. M. A., and Tavares, T. M.: Concentrations and species composition of atmospheric volatile organic compounds (VOCs) as observed during the wet and dry season in Rondônia (Amazonia), *Journal of Geophysical Research: Atmospheres*, 107, LBA 20–1–LBA 20–13, <https://doi.org/https://doi.org/10.1029/2000JD000267>, 2002.
- King, G. M. and Hungria, M.: Soil-atmosphere CO exchanges and microbial biogeochemistry of CO transformations in a Brazilian agricultural ecosystem, *Applied and environmental microbiology*, 68, 4480–4485, 2002.
- 530 Lan, X., Tans, P., Thoning, K., and NOAA Global Monitoring Laboratory: Trends in globally-averaged CO₂ determined from NOAA Global Monitoring Laboratory measurements., <https://doi.org/10.15138/9NOH-ZH07>, 2023.
- Laothawornkitkul, J., Taylor, J. E., Paul, N. D., and Hewitt, C. N.: Biogenic volatile organic compounds in the Earth system, *New Phytologist*, 183, 27–51, <https://doi.org/https://doi.org/10.1111/j.1469-8137.2009.02859.x>, 2009.
- 535 Lee, H., Rahn, T., and Throop, H.: An accounting of C-based trace gas release during abiotic plant litter degradation, *Global Change Biology*, 18, 1185–1195, 2012.
- Levin, I., Born, M., Cuntz, M., Langendörfer, U., Mantsch, S., Naegler, T., Schmidt, M., Varlagin, A., Verclas, S., and Wagenbach, D.: Observations of atmospheric variability and soil exhalation rate of radon-222 at a Russian forest site: Technical approach and deployment for boundary layer studies, *Tellus B: Chemical and Physical Meteorology*, <https://doi.org/10.3402/tellusb.v54i5.16681>, 2002.
- 540 Levin, I., Schmithüsen, D., and Vermeulen, A.: Assessment of ²²²radon progeny loss in long tubing based on static filter measurements in the laboratory and in the field, *Atmospheric Measurement Techniques*, 10, 1313–1321, <https://doi.org/10.5194/amt-10-1313-2017>, 2017.
- Lichtenthaler, H. K.: THE 1-DEOXY-D-XYLULOSE-5-PHOSPHATE PATHWAY OF ISOPRENOID BIOSYNTHESIS IN PLANTS, *Annual Review of Plant Physiology and Plant Molecular Biology*, 50, 47–65, <https://doi.org/10.1146/annurev.arplant.50.1.47>, PMID: 15012203, 1999.
- 545 Liu, L., Zhuang, Q., Zhu, Q., Liu, S., Van Asperen, H., and Pihlatie, M.: Global soil consumption of atmospheric carbon monoxide: an analysis using a process-based biogeochemistry model, *Atmospheric Chemistry and Physics*, 18, 7913–7931, 2018.
- Machado, L. and all: How the Amazonian Forest Produces New Particles, Submitted to *Nature*, XX, XX, 2023.
- 550 Machado, L. A. T., Franco, M. A., Kremper, L. A., Ditas, F., Andreae, M. O., Artaxo, P., Cecchini, M. A., Holanda, B. A., Pöhlker, M. L., Saraiva, I., Wolff, S., Pöschl, U., and Pöhlker, C.: How weather events modify aerosol particle size distributions in the Amazon boundary layer, *Atmospheric Chemistry and Physics*, 21, 18 065–18 086, <https://doi.org/10.5194/acp-21-18065-2021>, 2021.
- Mendonça, A. C., Dias-Júnior, C. Q., Acevedo, O. C., Santana, R. A., Costa, F. D., Negrón-Juarez, R. I., Manzi, A. O., Trumbore, S. E., and Marra, D. M.: Turbulence regimes in the nocturnal roughness sublayer: Interaction with deep convection and tree mortality in the Amazon, *Agricultural and Forest Meteorology*, 339, 109 526, 2023.
- 555 Mikkilä, C., Sundh, I., Svensson, B. H., and Nilsson, M.: Diurnal variation in methane emission in relation to the water table, soil temperature, climate and vegetation cover in a Swedish acid mire, *Biogeochemistry*, 28, 93–114, 1995.
- Moran-Zuloaga, D., Ditas, F., Walter, D., Saturno, J., Brito, J., Carbone, S., Chi, X., Hrabě de Angelis, I., Baars, H., Godoi, R. H. M., Heese, B., Holanda, B. A., Lavrič, J. V., Martin, S. T., Ming, J., Pöhlker, M. L., Ruckteschler, N., Su, H., Wang, Y., Wang, Q., Wang, Z., Weber, B., Wolff, S., Artaxo, P., Pöschl, U., Andreae, M. O., and Pöhlker, C.: Long-term study on coarse mode aerosols in the



- 560 Amazon rain forest with the frequent intrusion of Saharan dust plumes, *Atmospheric Chemistry and Physics*, 18, 10 055–10 088, <https://doi.org/10.5194/acp-18-10055-2018>, 2018.
- Nazaroff, W. W.: Radon transport from soil to air, *Reviews of Geophysics*, 30, 137–160, <https://doi.org/https://doi.org/10.1029/92RG00055>, 1992.
- Niinemets, : Photosynthesis and resource distribution through plant canopies, *Plant, Cell & Environment*, 30, 1052–1071, <https://doi.org/https://doi.org/10.1111/j.1365-3040.2007.01683.x>, 2007.
- 565 Nisbet, E. G., Manning, M. R., Dlugokencky, E. J., Fisher, R. E., Lowry, D., Michel, S. E., Myhre, C. L., Platt, S. M., Allen, G., Bousquet, P., Brownlow, R., Cain, M., France, J. L., Hermansen, O., Hossaini, R., Jones, A. E., Levin, I., Manning, A. C., Myhre, G., Pyle, J. A., Vaughn, B. H., Warwick, N. J., and White, J. W. C.: Very Strong Atmospheric Methane Growth in the 4 Years 2014–2017: Implications for the Paris Agreement, *Global Biogeochemical Cycles*, 33, 318–342, <https://doi.org/https://doi.org/10.1029/2018GB006009>, 2019.
- 570 Nölscher, A. C., Yañez-Serrano, A. M., Wolff, S., de Araujo, A. C., Lavrič, J. V., Kesselmeier, J., and Williams, J.: Unexpected seasonality in quantity and composition of Amazon rainforest air reactivity, *Nature Communications*, 7, 10 383, <https://doi.org/10.1038/ncomms10383>, 2016.
- Panov, A. V., Prokushkin, A. S., Kubler, K., Korets, M. A., Urban, A. V., Zrazhevskaya, G. K., Bondar', M. G., Heimann, M., and Zaehle, S.: Precise Observations of Atmospheric Carbon Dioxide and Methane Mole Fractions in the Polar Belt of Near-Yenisei Siberia, *Russian Meteorology and Hydrology*, 47, 829–838, <https://doi.org/10.3103/S1068373922110024>, 2022.
- 575 Pedruzo-Bagazgoitia, X., Patton, E. G., Moene, A. F., Ouwersloot, H. G., Gerken, T., Machado, L. A. T., Martin, S. T., Sörgel, M., Stoy, P. C., Yamasoe, M. A., and Vilà-Guerau de Arellano, J.: Investigating the Diurnal Radiative, Turbulent, and Biophysical Processes in the Amazonian Canopy-Atmosphere Interface by Combining LES Simulations and Observations, *Journal of Advances in Modeling Earth Systems*, 15, e2022MS003 210, <https://doi.org/https://doi.org/10.1029/2022MS003210>, e2022MS003210 2022MS003210, 2023.
- 580 Pfannerstill, E. Y., Reijrink, N. G., Edtbauer, A., Ringsdorf, A., Zannoni, N., Araújo, A., Ditas, F., Holanda, B. A., Sá, M. O., Tsokankunku, A., Walter, D., Wolff, S., Lavrič, J. V., Pöhlker, C., Sörgel, M., and Williams, J.: Total OH reactivity over the Amazon rainforest: variability with temperature, wind, rain, altitude, time of day, season, and an overall budget closure, *Atmospheric Chemistry and Physics*, 21, 6231–6256, <https://doi.org/10.5194/acp-21-6231-2021>, 2021.
- 585 Pöhlker, M. L., Pöhlker, C., Ditas, F., Klimach, T., Hrabec de Angelis, I., Araújo, A., Brito, J., Carbone, S., Cheng, Y., Chi, X., Ditz, R., Gunthe, S. S., Kesselmeier, J., Könemann, T., Lavrič, J. V., Martin, S. T., Mikhailov, E., Moran-Zuloaga, D., Rose, D., Saturno, J., Su, H., Thalman, R., Walter, D., Wang, J., Wolff, S., Barbosa, H. M. J., Artaxo, P., Andreae, M. O., and Pöschl, U.: Long-term observations of cloud condensation nuclei in the Amazon rain forest – Part I: Aerosol size distribution, hygroscopicity, and new model parametrizations for CCN prediction, *Atmospheric Chemistry and Physics*, 16, 15 709–15 740, <https://doi.org/10.5194/acp-16-15709-2016>, 2016.
- 590 Ravishankara, A. R.: Heterogeneous and Multiphase Chemistry in the Troposphere, *Science*, 276, 1058–1065, 1997.
- Rigby, M., Montzka, S. A., Prinn, R. G., White, J. W. C., Young, D., O'Doherty, S., Lunt, M. F., Ganesan, A. L., Manning, A. J., Simmonds, P. G., Salameh, P. K., Harth, C. M., Mühle, J., Weiss, R. F., Fraser, P. J., Steele, L. P., Krummel, P. B., McCulloch, A., and Park, S.: Role of atmospheric oxidation in recent methane growth, *Proceedings of the National Academy of Sciences*, 114, 5373–5377, <https://doi.org/10.1073/pnas.1616426114>, 2017.
- 595 Ringsdorf, A., Edtbauer, A., Vilà-Guerau de Arellano, J., Pfannerstill, E. Y., Gromov, S., Kumar, V., Pozzer, A., Wolff, S., Tsokankunku, A., Soergel, M., Sá, M. O., Araújo, A., Ditas, F., Poehlker, C., Lelieveld, J., and Williams, J.: Inferring the diurnal variability of OH



- radical concentrations over the Amazon from BVOC measurements, *Scientific Reports*, 13, 14900, <https://doi.org/10.1038/s41598-023-41748-4>, 2023.
- 600 Rohmer, M., Knani, M., Simonin, P., Sutter, B., and Sahm, H.: Isoprenoid biosynthesis in bacteria: a novel pathway for the early steps leading to isopentenyl diphosphate, *Biochemical Journal*, 295, 517–524, <https://doi.org/10.1042/bj2950517>, 1993.
- Rohmer, M., Seemann, M., Horbach, S., Bringer-Meyer, S., and Sahm, H.: Glyceraldehyde 3-Phosphate and Pyruvate as Precursors of Isoprenic Units in an Alternative Non-mevalonate Pathway for Terpenoid Biosynthesis, *Journal of the American Chemical Society*, 118, 2564–2566, <https://doi.org/10.1021/ja9538344>, 1996.
- 605 Rossabi, S., Choudoir, M., Helmig, D., Hueber, J., and Fierer, N.: Volatile Organic Compound Emissions From Soil Following Wet-ting Events, *Journal of Geophysical Research: Biogeosciences*, 123, 1988–2001, <https://doi.org/https://doi.org/10.1029/2018JG004514>, 2018.
- Rottenberger, S., Kuhn, U., Wolf, A., Schebeske, G., Oliva, S. T., Tavares, T. M., and Kesselmeier, J.: EXCHANGE OF SHORT-CHAIN ALDEHYDES BETWEEN AMAZONIAN VEGETATION AND THE ATMOSPHERE, *Ecological Applications*, 14, 247–262, <https://doi.org/https://doi.org/10.1890/01-6027>, 2004.
- 610 Rudolf, J. D., Alsup, T. A., Xu, B., and Li, Z.: Bacterial terpenome, *Nat. Prod. Rep.*, 38, 905–980, <https://doi.org/10.1039/D0NP00066C>, 2021.
- Rummel, U., Ammann, C., Gut, A., Meixner, F. X., and Andreae, M. O.: Eddy covariance measurements of nitric oxide flux within an Amazonian rain forest, *Journal of Geophysical Research: Atmospheres*, 107, LBA 17–1–LBA 17–9, <https://doi.org/https://doi.org/10.1029/2001JD000520>, 2002.
- 615 Schade, G. W., HOFMANN, R.-M., and CRUTZEN, P. J.: CO emissions from degrading plant matter., *Tellus B*, 51, 889–908, <https://doi.org/10.1034/j.1600-0889.1999.t01-4-00003.x>, 1999.
- Schaefer, H., Fletcher, S. E. M., Veidt, C., Lassey, K. R., Brailsford, G. W., Bromley, T. M., Dlugokencky, E. J., Michel, S. E., Miller, J. B., Levin, I., Lowe, D. C., Martin, R. J., Vaughn, B. H., and White, J. W. C.: A 21st-century shift from fossil-fuel to biogenic methane emissions indicated by $\delta^{13}\text{C}_{\text{CH}_4}$, *Science*, 352, 80–84, <https://doi.org/10.1126/science.aad2705>, 2016.
- 620 Seiler, W. and Conrad, R.: Contribution of tropical ecosystems to the global budget of trace gases, especially CH₄, H₂, CO, and N₂., R. E. Dickinson. John Wiley, New York, pp, pp. 133–160, 1987.
- Shlanta, A. and Moore, C. B.: Ozone and point discharge measurements under thunderclouds, *Journal of Geophysical Research*, 77, 4500–4510, <https://doi.org/10.1029/jc077i024p04500>, 1972.
- Sigler, J. M., Fuentes, J. D., Heitz, R. C., Garstang, M., and Fisch, G.: Ozone dynamics and deposition processes at a deforested site in the Amazon basin, *Ambio*, 31, 21–27, <https://doi.org/10.1579/0044-7447-31.1.21>, 2002.
- 625 Sivy, T. L., Shirk, M. C., and Fall, R.: Isoprene synthase activity parallels fluctuations of isoprene release during growth of *Bacillus subtilis*, *Biochemical and Biophysical Research Communications*, 294, 71–75, [https://doi.org/https://doi.org/10.1016/S0006-291X\(02\)00435-7](https://doi.org/https://doi.org/10.1016/S0006-291X(02)00435-7), 2002.
- Tarr, M. A., Miller, W. L., and Zepp, R. G.: Direct carbon monoxide photoproduction from plant matter, *Journal of Geophysical Research: Atmospheres* (1984–2012), 100, 11403–11413, 1995.
- 630 Thoning, K., Dlugokencky, E., Lan, X., and NOAA Global Monitoring Laboratory: Trends in globally-averaged CH₄, N₂O, and SF₆, <https://doi.org/10.15138/P8XG-AA10>, 2022.
- van Asperen, H., Warneke, T., Sabbatini, S., Nicolini, G., Papale, D., and Notholt, J.: The role of photo- and thermal degradation for CO₂ and CO fluxes in an arid ecosystem, *Biogeosciences*, 12, 4161–4174, <https://doi.org/10.5194/bg-12-4161-2015>, 2015.



- 635 van Asperen, H., Warneke, T., Carioca de Araújo, A., Forsberg, B., José Filgueiras Ferreira, S., Röckmann, T., van der Veen, C., Bulthuis, S., Ramos de Oliveira, L., de Lima Xavier, T., da Mata, J., de Oliveira Sá, M., Ricardo Teixeira, P., Andrews de França e Silva, J., Trumbore, S., and Notholt, J.: The emission of CO from tropical rain forest soils, *EGUsphere*, 2023, 1–29, <https://doi.org/10.5194/egusphere-2023-2746>, 2023.
- 640 Wang, J., Krejci, R., Giangrande, S., Kuang, C., Barbosa, H. M., Brito, J., Carbone, S., Chi, X., Comstock, J., Ditas, F., Lavric, J., Manninen, H. E., Mei, F., Moran-Zuloaga, D., Pöhlker, C., Pöhlker, M. L., Saturno, J., Schmid, B., Souza, R. A., Springston, S. R., Tomlinson, J. M., Toto, T., Walter, D., Wimmer, D., Smith, J. N., Kulmala, M., Machado, L. A., Artaxo, P., Andreae, M. O., Petäjä, T., and Martin, S. T.: Amazon boundary layer aerosol concentration sustained by vertical transport during rainfall, *Nature*, 539, 416–419, <https://doi.org/10.1038/nature19819>, 2016.
- 645 Williams, E., Rosenfeld, D., Madden, N., Gerlach, J., Gears, N., Atkinson, L., Dunnemann, N., Frostrom, G., Antonio, M., Biazon, B., Camargo, R., Franca, H., Gomes, A., Lima, M., Machado, R., Manhaes, S., Nachtigall, L., Piva, H., Quintiliano, W., Machado, L., Artaxo, P., Roberts, G., Renno, N., Blakeslee, R., Bailey, J., Boccippio, D., Betts, A., Wolff, D., Roy, B., Halverson, J., Rickenbach, T., Fuentes, J., and Avelino, E.: Contrasting convective regimes over the Amazon: Implications for cloud electrification, *Journal of Geophysical Research: Atmospheres*, 107, LBA 50–1–LBA 50–19, <https://doi.org/https://doi.org/10.1029/2001JD000380>, 2002.
- 650 Williams, J., Fischer, H., Hoor, P., Pöschl, U., Crutzen, P., Andreae, M., and Lelieveld, J.: The influence of the tropical rainforest on atmospheric CO and CO₂ as measured by aircraft over Surinam, South America, *Chemosphere - Global Change Science*, 3, 157–170, [https://doi.org/10.1016/s1465-9972\(00\)00047-7](https://doi.org/10.1016/s1465-9972(00)00047-7), 2001.
- Winderlich, J., Chen, H., Höfer, A., Gerbig, C., Seifert, T., Kolle, O., Kaiser, C., Lavrič, J., and Heimann, M.: Continuous low-maintenance CO₂/CH₄/H₂O measurements at the Zotino Tall Tower Observatory (ZOTTO) in Central Siberia, *Atmospheric Measurement Techniques Discussions*, 3, 1399–1437, 2010.
- 655 Yáñez Serrano, A. M., Nölscher, A. C., Williams, J., Wolff, S., Alves, E., Martins, G. A., Bourtsoukidis, E., Brito, J., Jardine, K., Artaxo, P., and Kesselmeier, J.: Diel and seasonal changes of biogenic volatile organic compounds within and above an Amazonian rainforest, *Atmospheric Chemistry and Physics*, 15, 3359–3378, <https://doi.org/10.5194/acp-15-3359-2015>, 2015.
- 660 Yanez-Serrano, A. M., Bourtsoukidis, E., Alves, E. G., Bauwens, M., Stavrou, T., Llusà, J., Filella, I., Guenther, A., Williams, J., Artaxo, P., Sindelarova, K., Doubalova, J., Kesselmeier, J., and Peñuelas, J.: Amazonian biogenic volatile organic compounds under global change, *Global Change Biology*, 26, 4722–4751, <https://doi.org/https://doi.org/10.1111/gcb.15185>, 2020.
- Yonemura, S., Morokuma, M., Kawashima, S., and Tsuruta, H.: Carbon monoxide photoproduction from rice and maize leaves, *Atmospheric Environment*, 33, 2915–2920, [https://doi.org/https://doi.org/10.1016/S1352-2310\(99\)00099-0](https://doi.org/https://doi.org/10.1016/S1352-2310(99)00099-0), 1999.
- 665 Zhao, Z., Zhang, W., Alexander, T., Zhang, X., Martin, D. B. C., and Zhang, H.: Isolating α -Pinene Ozonolysis Pathways Reveals New Insights into Peroxy Radical Chemistry and Secondary Organic Aerosol Formation, *Environmental Science & Technology*, 55, 6700–6709, <https://doi.org/10.1021/acs.est.1c02107>, 2021.